Fermi National Accelerator Laboratory

TM-1693

Experimental Study of the Main Ring Transition Crossing *

Ioanis Kourbanis, Keith Meisner and King-Yuen Ng
Fermi National Accelerator Laboratory
P.O. Box 500
Batavia, Illinois 60510

October 1990

* Submitted to the proceedings of the Fermilab III Instabilities Workshop, St. Charles, Illinois, June 25-29, 1990.

Operated by Universities Research Association Inc. under contract with the United States Department of Energy

EXPERIMENTAL STUDY OF THE MAIN RING TRANSITION CROSSING

Ioanis Kourbanis, Keith Meisner, and King-Yuen Ng

Fermi National Accelerator Laboratory, P.O. Box 500, Batavia, IL 60510*

1. Introduction

A number of different experiments were proposed as part of the Fermilab III Instabilities Workshop in order to study the transition crossing in the Main Ring. Due to time limitations and operational restrictions only one of the experiments was actually performed. The results and analysis presented here are preliminary. We used an injection mismatch to deliberately blow up the longitudinal emittance in the MR 29 cycles, and measured the increase in bunch emittance and the particle loss through transition as functions of the initial bunch emittance. The experiment was repeated for different intensities (2, 4 booster turns) and for different rf voltages around transition. The purpose of the experiment was to distinguish the mechanism that is responsible for emittance growth and particle loss across transition.

Two mechanisms can lead to the growth of bunch emittance and particle loss across transition. The first one is nonlinearity, which is due to the nonlinear terms in the expansion of the momentum compaction factor or the orbit length as a power series in the momentum spread. With these nonlinear terms, particles of different momenta cross transition at different times. The spread in crossing time is called the *nonlinear time*,[1] which is proportional to the momentum spread and depends on the Johnsen's nonlinear coefficient[2] in the momentum compaction factor. After those particles with larger momenta than the synchronous particle cross transition and before the rf phase is switched, they are outside the accelerating bucket and drift away forming a tail in the longitudinal phase space. Those particles with lower momenta than the synchronous particle also develop into a tail after the rf phase is switched because they cross transition much later. These tails can lead to emittance growth and particle loss. The second mechanism is microwave instability because the

*Operated by the Universities Research Association, Inc., under contract with the U.S. Department of Energy.

phase-slip parameter $\eta = 1/\gamma_T^2 - 1/\gamma^2$ is vanishingly small near transition and therefore cannot provide enough Landau damping to stabilize the growth of the microwave amplitudes. However, these two mechanisms are very different.

If nonlinear effect dominates at transition crossing, we expect the effect to increase with initial bunch emittance ϵ_L and the rf voltage $V_{\rm rf}$ at transition. This is because a bigger ϵ_L or a bigger $V_{\rm rf}$ at constant $\dot{\gamma}_T$ implies larger momentum spread, which enhances the time difference between the fastest particle and the synchronous particle in crossing transition. In fact, according to Ref. 1, we have

$$\frac{\Delta\epsilon_L}{\epsilon_L} \propto \epsilon_L^{\frac{1}{2}} V_{\rm rf}^{\frac{2}{3}} \ . \tag{1}$$

On the other hand, if microwave instability dominates at transition crossing, we expect its effect to decrease with initial bunch emittance and rf voltage at transition. This is because both larger ϵ_L and $V_{\rm rf}$ imply larger momentum spread near transition, which in turn provides more Landau damping for stabilization. We obtain from Refs. 3 and 4 that

$$\frac{\Delta\epsilon_L}{\epsilon_L} \propto \epsilon_L^{-3} V_{\rm rf}^{-1} \ . \tag{2}$$

When the bunch emittance is sufficiently small, the dominant effect should be microwave instability. However, when the bunch emittance is sufficiently large, nonlinearity should dominate. As a result, we expect to see the variations of emittance growth and particle loss as functions of initial bunch emittance to follow curves as indicated in Fig. 1. Also microwave effect is intensity dependent while nonlinear effect is not.

2. Preparation and setup

We found that the most effective way to increase the emittance at injection in the MR was through phase mismatch. We started with 0° phase error and tuned the rf voltage at injection so as to minimize the bunch length oscillations measured by the BLMON, a bunch-length monitor which is not well-calibrated. A picture of BLMON, rf voltage RFSUMT, rf phase PHIS, and radial beam position RPOSP at injection after the tuning is shown on Fig. 2. The absence of synchrotron oscillations before transition was checked by taking mountain range pictures at 0.32 sec into the cycle

i.e., 60 ms before transition. Fig. 3 shows a typical mountain range picture taken during our studies. It shows 30 traces 10 turns (0.2 ms) apart.

The longitudinal emittance was calculated by measuring the bunch length (from mountain range pictures), the rf voltage and the rf phase at two places before transition (60, 30 ms) and at two places after transition (60, 150 ms). Figure 4 shows a picture of two beam profiles before and two after transition for 2 booster cycles and 150° phase mismatch. The particle loss through transition was measured with the intensity monitor IBEAMM.

Figure 5 shows a typical picture of the rf voltage RFSUMT, the beam intensity IBEAMM, the radial position RPOSP and the phase angle PHIS in the time interval we took our measurements. An injection phase error was then introduced and the measurements were repeated. The phase error varied between 0° and 40°. As mentioned before, measurements were taken at two different intensities, i.e., for 2, 4 booster turns corresponding to 0.9×10^{10} and 1.6×10^{10} ppb respectively.

Efforts had also been made to blow up the bunch emittance by introducing a rf-voltage mismatch, but the blowup was not as efficient as the phase mismatch. The bunch spreader had also been used. In this case, the output bunch shape became so irregular that the bunch length was unable to be defined.

3. Results and Conclusions

The results of our experiment are summarized in Figs. 6 and 7, where we have plotted the growth in bunch area and particle loss through transition as functions of the initial emittance for two different intensities and two transition voltages. The errors indicate mainly the uncertainty in estimating the the bunch length.

Figures 6(a), 6(b), 7(a), and 7(b) show clearly that both the fractional growth in emittance and particle loss increase with V_{rf} at transition. As a result, we conclude that nonlinear effect dominates the Main Ring at transition.

We see from Figs. 6(b) and 7(b) that particle loss also increases with the initial bunch emittance ϵ_L as expected in a nonlinear-effect dominance. However, a closer look at Figs. 6(a) and 7(a) reveals that the fractional growth in emittance stays roughly constant with the initial bunch emittance at $V_{rf} = 2.0$ MV for 4-booster-turn

injection, and even decreases slightly with ϵ_L at both $V_{rf} = 2.0$ MV and 2.3 MV for 2-booster-turn injection. The 4-booster-turn results are understandable. A $\Delta\epsilon_L/\epsilon_L$ constant with ϵ_L at $V_{rf} = 2.0$ MV implies that there is some contribution from microwave instability. At $V_{rf} = 2.3$ MV, the bunch becomes much more microwave stable and therefore $\Delta\epsilon_L/\epsilon_L$ increases with ϵ_L due to nonlinear effect in the region 0.15 eV-sec $< \epsilon_L <$ 0.23 eV-sec. In the same ϵ_L region and at the same V_{rf}, a 2-booster-turn (lower intensity) bunch should be much less affected by microwave growth than a 4-booster-turn bunch. We should expect more nonlinearity dominance so that the fractional growth of emittance should increase more rapidly with ϵ_L than the 4-booster-turn results. However, as depicted in Fig. 6(a) the fractional growth of emittance decreased slightly with ϵ_L instead. This contradiction may arise from errors in the measurement.

Quantitatively, we find that for 2-turn fixed intensity (0.9×10^{10} ppb) the growth of bunch area was about 10% and did not change much when the voltage around transition varied from from 2.0 to 2.3 MV. For the larger intensity (1.6×10^{10} ppb), the bunch area growths were about 40% and 60%, respectively, for the two rf voltages. The particle loss followed an exponential increase and grew must faster for larger transition voltage. Numerical fittings gives

$$\% \text{ Particle Loss} = \begin{cases} 0.0139e^{24.7\epsilon_L} & \text{2 turn at 2.0 MV ,} \\ 0.0765e^{20.9\epsilon_L} & \text{2 turn at 2.3 MV ,} \\ 0.178e^{14.3\epsilon_L} & \text{4 turn at 2.0 MV ,} \\ 0.482e^{13.1\epsilon_L} & \text{4 turn at 2.3 MV .} \end{cases} \tag{3}$$

REFERENCES

1. J. Wei, *Transition Crossing in the Main Injector*, these proceedings.

2. K. Johnsen, *Effects on Nonlinearities on Phase Transition*, CERN, Symposium on High Energy Accelerators, Geneva, 1956, Vol. 1, p.106.

3. S.Y. Lee and J.M. Wang, IEEE Tranc. Nucl. Sc. **NS 32**, 2323 (1985).

4. K.Y. Ng, *Some Estimation Concerning Crossing Transition of the Main Injector*, FNAL-TM1670, 1990, also these proceedings.

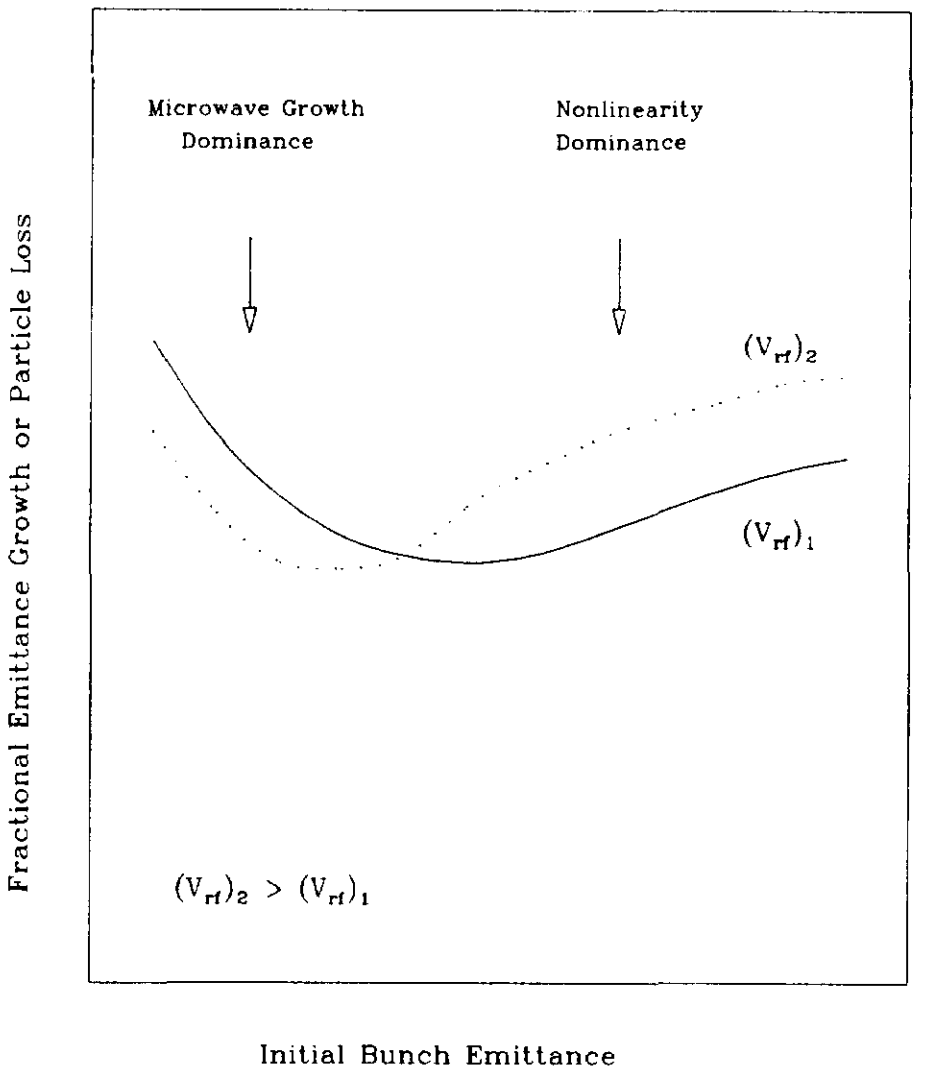

Figure 1

Schematic plot of fractional growth of bunch emittance and particle loss across transition versus initial bunch emittance at different transition rf voltages.

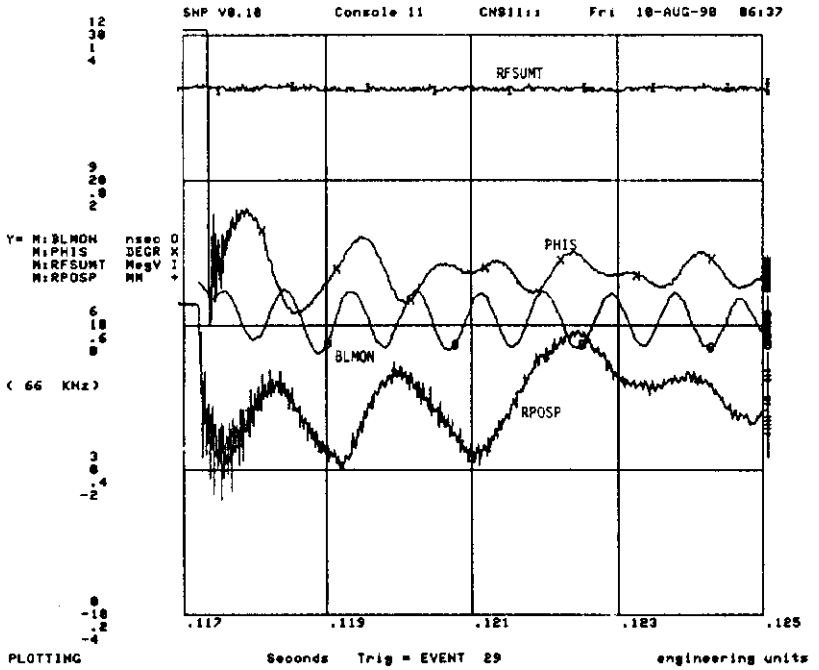

Figure 2

Typical bunch length oscillations, rf voltage synchronous phase and radial position at injection in a 29 cycle (4 booster turns no phase error).

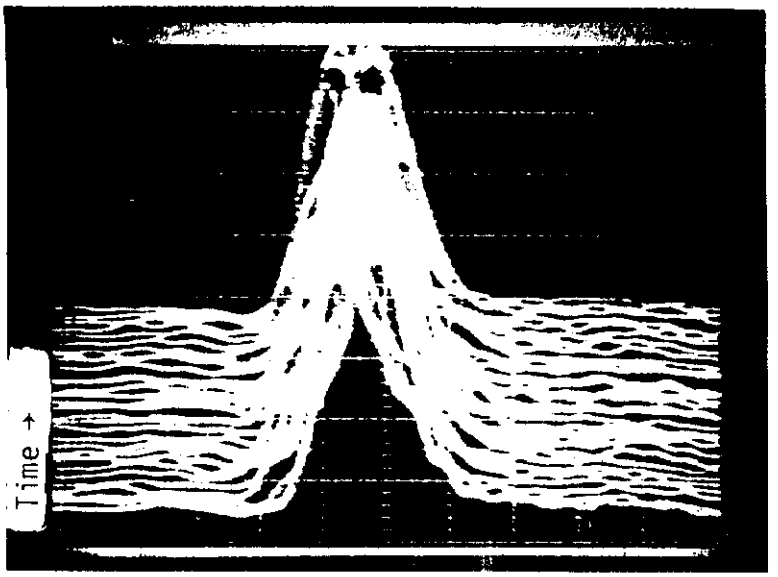

Figure 3

Typical mountain range picture before transition (30 traces 10 turns or 0.2 msec apart).

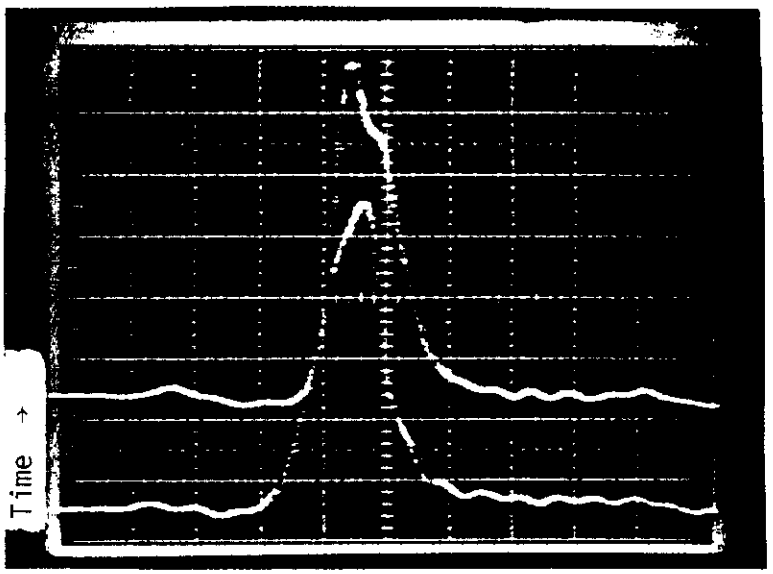

Figure 4(a)

Beam profile 60 ms and 30 ms before transition for 2 booster cycles and 150° phase mismatch.

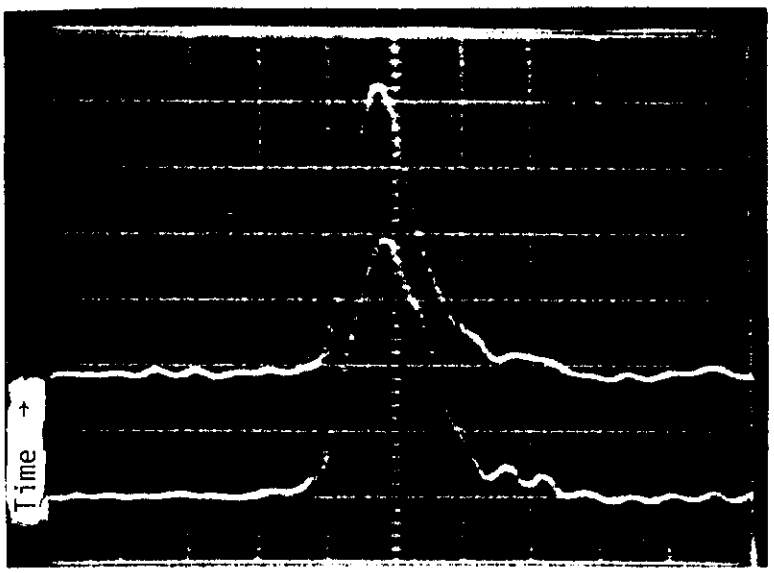

Figure 4(b)

Beam profile 60 ms and 150 ms after transition for 2 booster cycles and 150° phase mismatch.

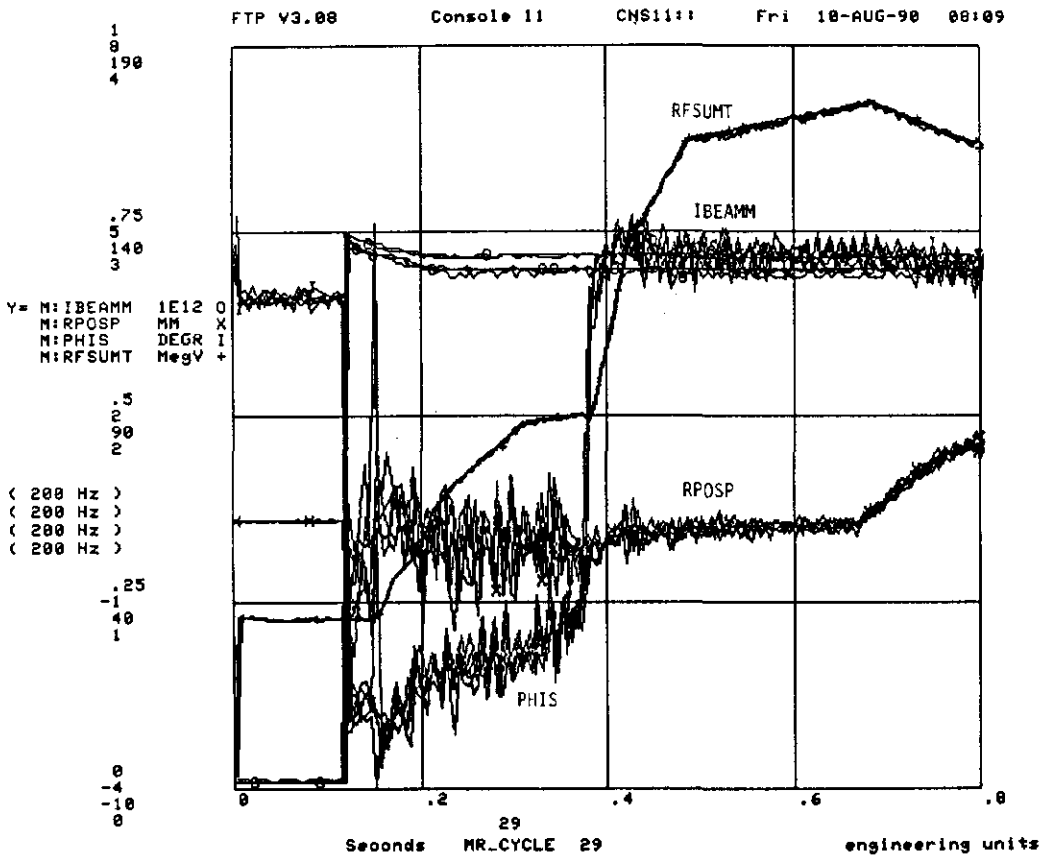

Figure 5

Typical picture of the beam intensity IBEAMM, rf voltage RFSUMT, radial position RPOSP, and synchronous phase PHIS versus time in a 29 cycle during our measurements.

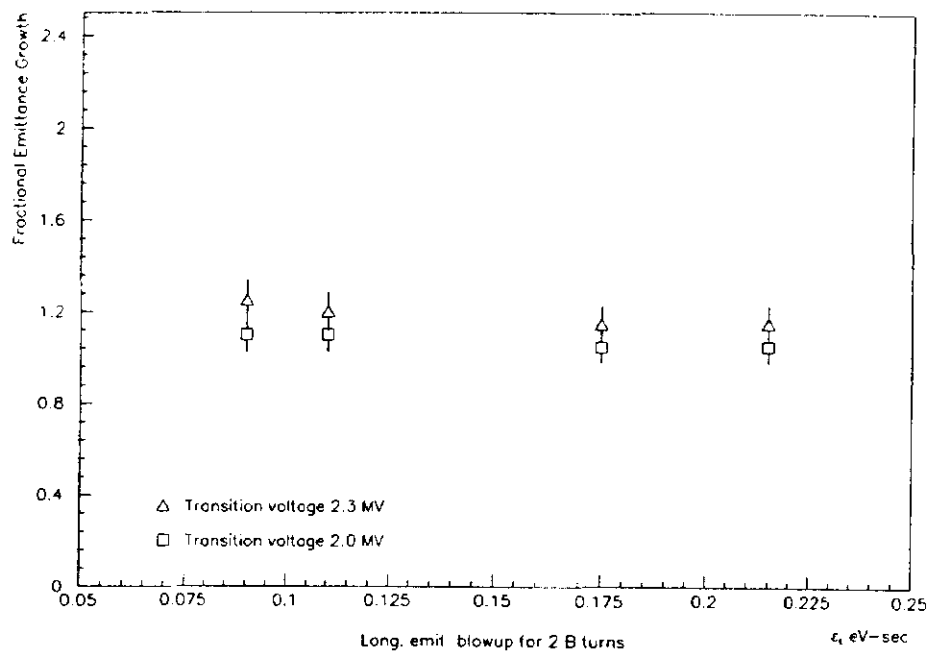

Figure 6(a)

Change in bunch area as a function of initial bunch emittance for 2 booster turns.

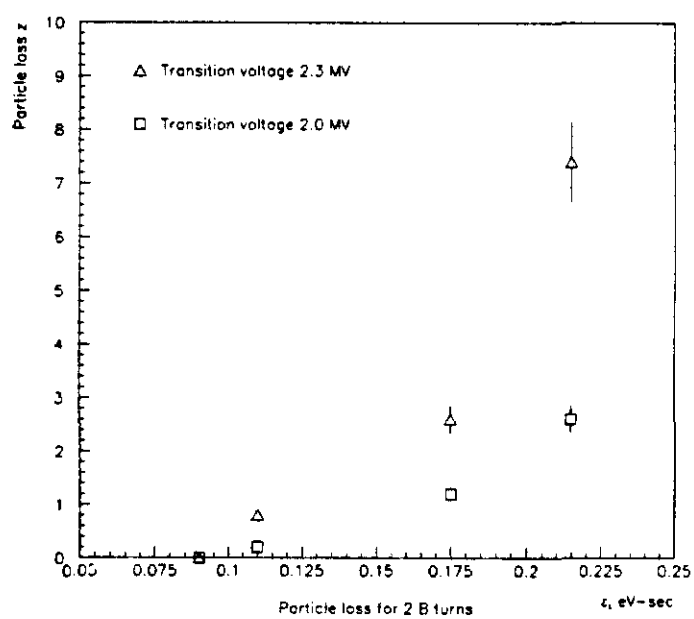

Figure 6(b)

Particle loss through transition versus initial bunch emittance for 2 booster turns.

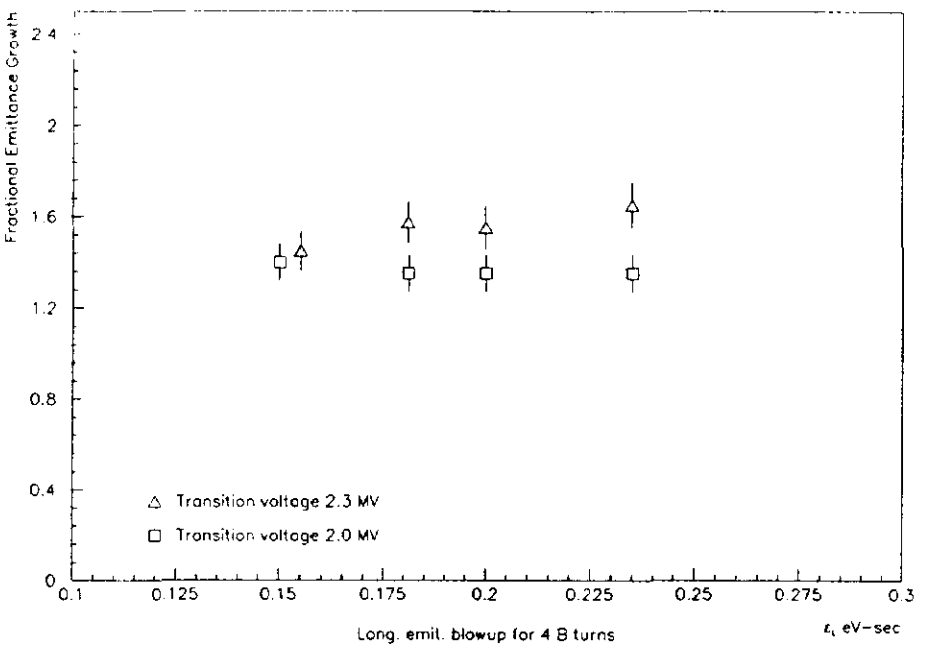

Figure 7(a)

Change in bunch area as a function of initial bunch emittance for 4 booster turns.

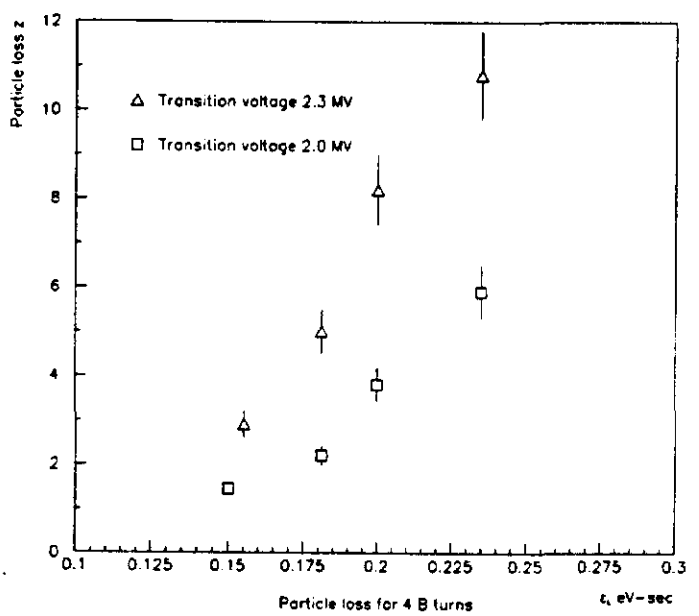

Figure 7(b)

Particle loss through transition versus initial bunch emittance for 4 booster turns.